Phase diagram of one-dimensional driven lattice gases with open boundaries

1998 J. Phys. A: Math. Gen. 31 6911

(http://iopscience.iop.org/0305-4470/31/33/003)

J. Phys. A: Math. Gen. **31** (1998) 6911–6919. Printed in the UK PII: S0305-4470(98)92448-9

Phase diagram of one-dimensional driven lattice gases with open boundaries

Anatoly B Kolomeisky†, Gunter M Schütz‡, Eugene B Kolomeisky§ and Joseph P Straley‖

† Department of Chemistry, Baker Laboratory, Cornell University, Ithaca, NY 14853-1301, USA
‡ IFF, Forschungszentrum Jülich, 52425 Jülich, Germany
§ Department of Physics, University of Virginia, Charlottesville, VA 22901, USA
‖ Department of Physics and Astronomy, University of Kentucky, Lexington, KY 40506-0055, USA

Received 13 March 1998

Abstract. We consider the asymmetric simple exclusion process (ASEP) with open boundaries and other driven stochastic lattice gases of particles entering, hopping and leaving a one-dimensional lattice. The long-term system dynamics, stationary states, and the nature of phase transitions between steady states can be understood in terms of the interplay of two characteristic velocities, the collective velocity and the shock (domain wall) velocity. This interplay results in two distinct types of domain walls whose dynamics is computed. We conclude that the phase diagram of the ASEP is generic for one-component driven lattice gases with a single maximum in the current-density relation.

1. Introduction

Driven lattice gases with open boundaries are stochastic lattice models of particles which hop preferentially in one direction and which are connected at their boundaries to particle reservoirs of constant densities. As a result of this coupling, a stationary particle current is maintained and the system never reaches an equilibrium state. A well known example, which has become one of the standard models of nonequilibrium statistical mechanics, is the asymmetric simple exclusion process (ASEP) where particles interact through hard-core exclusion. This model is relevant to a variety of phenomena in physics and beyond [1]. The one-dimensional version of this model was first introduced in 1968 to provide a qualitative understanding of the kinetics of protein synthesis on RNA templates in terms of a 'traffic jam' of ribosomes along the RNA [2, 3]. Other open systems in which transport of hard-core particles through narrow (i.e. essentially one-dimensional) channels has been observed in more recent experiments include certain types of zeolites [4]. Also recently, generalized ASEPs have been succesfully used in traffic flow modelling [5]. On the mathematical side [6, 7], the system is of interest in the theory of interacting particle systems because of its tractability in conjunction with its rich and nontrivial behaviour.

The one-dimensional ASEP with open boundaries shows a complex behaviour exhibiting nonequilibrium phase transitions that have no analogues in thermal equilibrium [1, 8] (see section 2). There are intuitive arguments and evidence from the study of related problems [7, 9, 10] that domain walls (shocks) and the nature of the boundary conditions imposed on the system play a central role in understanding the physics of the system. The quantitative

0305-4470/98/336911+09$19.50

clarification and development of the domain wall picture for the system with open boundaries [11] constitute the primary goal of this paper. The totally asymmetric exclusion process (TASEP) is the simplest case and we shall use this model to develop a theory of boundary-induced phase transitions (section 3). The central ingredient of this theory is an interplay of two characteristic shock velocities which can be derived from the (bulk) current density relation $j(\rho)$. We are lead to the observation of *two different* types of domain walls whose structure and motion can be characterized to a large extent. The system dynamics, stationary states, the nature and the location of the phase transitions can then be understood *quantitatively* in terms of the domain wall picture. The basic mechanisms which generate the phase transitions in this model will be shown to be universal and will thus eventually lead us to an understanding of more generic cases of driven diffusive systems which have a single maximum in the current density relation $j(\rho)$. Moreover, we shall obtain—with somewhat stronger assumptions on the coarse-grained domain wall dynamics—quantitative results on the stationary density profile close to the phase transition lines (section 4). Some further conclusions are drawn in section 5 where we also summarize our main results.

2. The TASEP with open boundaries

In the TASEP particles enter an N-site lattice from the left with rate α whenever the first site is empty. In the bulk particles can jump to the neighbouring right-hand site with constant rate 1 provided that this site is empty (hard-core exclusion). On site N particles exit the system with rate β. This choice of rates corresponds to a coupling of the system to reservoirs of constant densities α and $1-\beta$, respectively. The steady states in this system (figure 1) have been determined exactly [11, 12]. For self-containedness we summarize the main results.

The hard-core exclusion implies that the steady state particle current j is related to the bulk density ρ by $j = \rho(1-\rho)$ [13]. When particles are supplied at the left end with the rate $\alpha > \beta$, and removed at the right end not too fast, $\beta < \frac{1}{2}$, there results a high-density

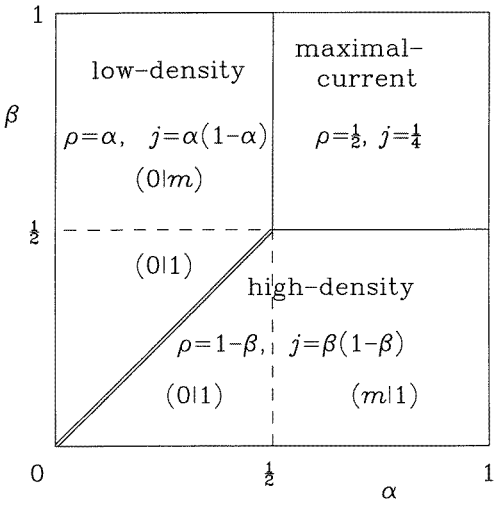

Figure 1. Phase diagram of the ASEP with stationary values of the particle density ρ, current j, and allowed types of domain walls: low-density/high-density (0|1), maximal-current/high-density (m|1), low-density/maximal-current (0|m).

phase (bulk density $\rho_{\text{high}} = 1-\beta > \frac{1}{2}$) for which particle extraction is the limiting process. When the particles are supplied not too fast, $\alpha < \frac{1}{2}$ and removed faster than supplied, $\beta > \alpha$, there results a low-density phase limited by particle supply; the bulk density is $\rho_{\text{low}} = \alpha$. There is a discontinuous phase transition along the line $\alpha = \beta < \frac{1}{2}$. Here the average particle density changes linearly across the system from α to $1-\alpha$. When particles are supplied and removed sufficiently rapidly, $\alpha > \frac{1}{2}$, $\beta > \frac{1}{2}$, there results a continuous phase transition into a maximal-current phase for which transport is bulk dominated; the bulk density is $\rho_m = \frac{1}{2}$, and the current takes on its maximal value of $\frac{1}{4}$.

Boundary density profiles in the high- and low-density phases decay exponentially with finite localization length ξ; the localization length diverges as the maximal current phase is entered. Within the maximal-current phase the decay is algebraic (equivalent to an infinite correlation length). Remarkably, ξ is composed of two individual localization lengths [11]

$$\xi^{-1} = |\xi_\beta^{-1} - \xi_\alpha^{-1}| \tag{1}$$

with $\xi_\sigma^{-1} = -\ln 4\sigma(1-\sigma)$ for $\sigma < \frac{1}{2}$ and $\xi_\sigma^{-1} = 0$ for $\sigma \geqslant \frac{1}{2}$. A curious implication of this equation is that the boundary density profile changes form within the high- and low-density phases (for example, at $\alpha = \frac{1}{2}$ with $\beta < \frac{1}{2}$), yet this is not accompanied by any nonanalyticity in the current or bulk density. Along the first order transition line $\alpha = \beta < \frac{1}{2}$ the correlation length ξ is infinite, but the individual localization lengths $\xi_{\alpha,\beta}$ are finite. The mean-field solution [2, 14] for the density on this line has the form of a shock front or domain wall, and the linear stationary state profile that is observed in the exact solution can be interpreted as a superposition of domain walls present at any position [11, 15, 16]. Excepting the special case of this coexistence line the nature and motion of the domain wall and the consequences for the phase diagram have not been elucidated generally and explicitly for the problem with open boundaries.

3. Domain wall dynamics

From the exact solution we realize that understanding the origin and the physical meaning of the localization lengths $\xi_{\alpha,\beta}$ holds the key to understanding the phase diagram of the system. We start from two examples that provide insight into the physics of the TASEP. Since the model has a particle–hole symmetry—it can be reformulated in terms of holes entering the system from the right end—we only need to study the region $\alpha \geqslant \beta$.

(1) Let us assume [16] that α and β are very small ($\alpha N \ll 1, \beta N \ll 1$) and that the initial distribution of particles is far from the true stationary state. The particles will travel to the right end where they get stuck. At late times there will be a low-density region at the left and a high-density region at the right (which we can present schematically as 00001111), with a domain wall between the low (0)- and high (1)-density segments. The subsequent late-stage evolution of the system can be interpreted in terms of the motion of this domain wall.

When a particle exits the system, the remaining particles rearrange themselves so that the whole filled region shrinks by one lattice unit, and the domain wall moves one step to the right. The conditions $\alpha N \ll 1$, $\beta N \ll 1$ guarantee that while this rearrangement takes place, no extra particle enters or leaves the system. Similarly a particle entering the system from the left causes the domain wall to move one unit to the left. As in the Zel'dovich theory of kinetics of first-order transitions [17], the domain wall motion can be understood as diffusion of the 'size of the high-density segment'. The 'elementary processes' that change the length of the filled region consist of motion of the domain wall to the left at rate

α or to the right at rate β, so that the domain wall does a biased random walk with drift velocity $V = \beta - \alpha$ and diffusion coefficient $D = (\alpha + \beta)/2$. As a result, three physically different situations are possible.

If $\alpha < \beta$, then the domain wall is drifting to the right and will eventually reach the end of the system; thereafter the system is in the low-density stationary state. If $\alpha > \beta$, the domain wall is travelling to the left, leading to the high-density stationary state. When $\alpha = \beta$, the domain wall position fluctuates with no net drift, and its rms displacement increases with time as $(Dt)^{1/2}$. Hence, at large times it can be anywhere in the system, resulting in a linearly increasing stationary density profile as suggested earlier for finite rates α, β on an intuitive basis. We note that following the dynamics of the wall also explains *why* the phase transition between the cases $\alpha > \beta$ and $\alpha < \beta$ is discontinuous.

(2) Let us now assume that $\alpha > \frac{1}{2}$ and that only β is very small. We start from an empty lattice. After a while, but before the true high-density stationary state is reached, the system consists of two visually different segments which can be presented schematically as mmmm1111. Near the left end of the system the high entering rate causes the formation of a region closely resembling the maximal-current phase (m), while on the right there is a high-density region (1) dominated by the small exit rate β. The expansion of the high-density segment is again a biased random walk with some drift velocity and diffusion coefficient, determined below.

In equilibrium phenomena a domain wall is a localized region where the order parameter interpolates between degenerate ground states. In this nonequilibrium system a domain wall is an object connecting two possible *stationary* states of the system. The domain wall picture exhibited in the two examples is not specific to the case that one of the boundary rates is small; we argue that everywhere in the low-/high-density phases there are two kinds of domain walls: the (0|1) wall (for $\alpha < \frac{1}{2}$) connecting the stable high-density stationary state to the metastable low-density state (as in example (1)), and the $(m|1)$ wall [for $\alpha > 1/2$] that connects the stable high-density stationary state to the maximal-current phase (example (2)). This second, distinct type of domain wall is a new notion that we need to introduce here for a full understanding of the system. The bulk densities far to the left and right (ρ_{low} and ρ_{high}, respectively) of the (0|1) domain wall are reached exponentially fast with length scale ξ. As we increase the entering rate α (holding the exit rate $\beta < \frac{1}{2}$ fixed), the localization length ξ_α characterizing the low-density behaviour of the domain wall increases, going to infinity [11, 12] at $\alpha = \frac{1}{2}$: The (0|1) wall undergoes a continuous phase transition into the maximal-current/high-density domain wall $(m|1)$ described in our second example. Because the maximal current phase is algebraic, the stationary density profile for $\alpha \geqslant \frac{1}{2}$ approaches its bulk value not *purely* exponentially, but with an algebraic correction. Thus the domain wall transition explains the non-analytical change of the stationary density profile within the high-density phase at $\alpha = \frac{1}{2}$ for any value of $\beta < \frac{1}{2}$.

We turn now to a quantitative analysis of the physical origin of these observations in terms of the drift velocity of the domain wall and of the collective velocity of the lattice gas, defined below. To this end we will now show how the late-stage dynamics of the system and the approach to the true high-density stationary state is governed by the motion of the two types of domain walls.

In the introductory examples the domain wall was easy to visualize because the wall is sharp when the entering and exit rates are small. To compute the drift velocity in the general case we first note that in any lattice gas (with conserved total particle number) the local particle density $\rho(x, t) = \langle n_x(t) \rangle$ satisfies a lattice continuity equation

$$\frac{\mathrm{d}}{\mathrm{d}t}\rho(x, t) = j_{x-1}(t) - j_x(t) \tag{2}$$

with the local particle current $j_x(t)$. In the continuum limit this turns into the usual continuity equation $\partial\rho/\partial t + \partial j/\partial x = 0$. With a travelling wave solution of the form $\rho(x - Vt)$, and integrating between minus and plus infinity, we find the domain wall velocity

$$V = \frac{j_+ - j_-}{\rho_+ - \rho_-}. \tag{3}$$

In a finite macroscopic system the assumption $\rho(x, t) = \rho(x - Vt)$ breaks down near the boundaries, and therefore the parameters $j_{+,-}$ and $\rho_{+,-}$ (given in figure 1) should be understood as bulk stationary state values of the current and density in the far left $(-)$ and far right (+) parts of the domain wall.

For the low-density/high-density domain wall (0|1) one has $j_+ = \beta(1-\beta)$, $\rho_+ = 1-\beta$, and $j_- = \alpha(1-\alpha)$, $\rho_- = \alpha$ (figure 1). Substituting these in (3) we find the drift velocity V for the TASEP

$$V = \beta - \alpha \tag{4}$$

which we expect to be valid for all $\alpha, \beta < \frac{1}{2}$ and which is a well-established result for the *infinite* system without boundaries [7, 13]. One realizes that the domain velocity changes sign at $\alpha = \beta < \frac{1}{2}$, leading to the same scenario as in example 1 for small α, β.

For the maximal-current/high-density domain wall $(m|1)$ we have $j_+ = \beta(1-\beta)$, $\rho_+ = 1-\beta$, and $j_- = \frac{1}{4}$, $\rho_- = \frac{1}{2}$. Hence for an initially empty lattice

$$V = \beta - \tfrac{1}{2}. \tag{5}$$

The expression for V changes its functional form at $\alpha = \frac{1}{2}$ because the wall has a different form beyond the phase transition $(0|1) \to (m|1)$.

To understand *why* the transition takes place at $\alpha = \frac{1}{2}$ we consider the collective velocity

$$V^{\mathrm{coll}} \equiv \frac{\mathrm{d}}{\mathrm{d}t} \frac{\sum_x x\langle n_x(t)(n_0(0) - \rho)\rangle}{\sum_x \langle n_x(n_0(0) - \rho)\rangle} \tag{6}$$

of a lattice gas, averaged over a translationally invariant grand-canonical stationary distribution of density ρ. The collective velocity measures the drift of the centre of mass of a momentary local perturbation of the stationary distribution. For any lattice gas satisfying a continuity equation (2) we obtain by taking the thermodynamic limit of a finite system the exact nonequilibrium fluctuation-dissipation theorem

$$V^{\mathrm{coll}} = \frac{\partial}{\partial\rho} j(\rho). \tag{7}$$

For the TASEP with $j = \rho(1-\rho)$ one finds $V^{\mathrm{coll}} = 1 - 2\rho$ which changes sign at $\rho = \frac{1}{2}$ where the current takes its maximal value $j = \frac{1}{4}$. As in traffic flow a small perturbation (e.g. an additional car which has just entered the road) will move with positive velocity (in the direction of the flow) if the overall density is sufficienty low. However, in a high-density regime, such a perturbation causes incoming particles to pile up behind the perturbation (traffic jam) and thus leads to a negative collective velocity of the centre of mass of the perturbation.

To appreciate the significance of the collective velocity for the phase diagram of the TASEP consider first the low-density phase along a line with fixed $\beta > \frac{1}{2}$. For a left boundary density $\alpha < \frac{1}{2}$ a small perturbation of the stationary state (corresponding to a fluctuation in the injection of particles) travels with positive speed into the bulk where it will eventually dissipate. However, if the perturbation is maintained, i.e. the constant left boundary density is increased by a small amount, the perturbation will continuously penetrate into the bulk and lead to an increase of the bulk density. This happens until

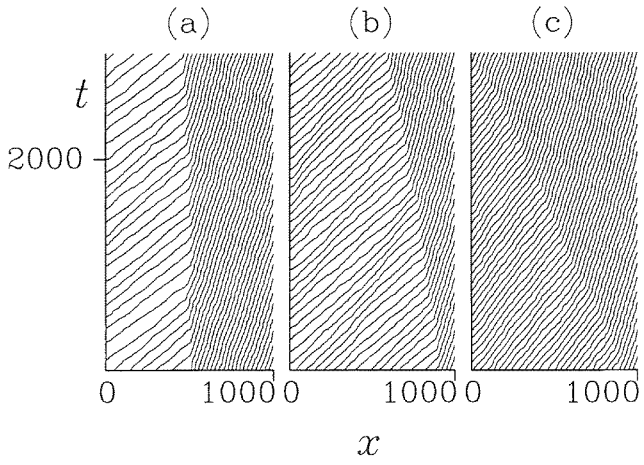

Figure 2. An ASEP with a domain wall present. The diagonal lines represent the instantaneous position x (measured in lattice spacings) of every 10th particle at various times t (measured in Monte Carlo steps per site). (a) $\alpha = \beta = 0.2$; (b) $\alpha = 0.3$, $\beta = 0.2$; (c) $\alpha = 0.7$, $\beta = 0.2$.

$\alpha = \frac{1}{2}$. Further increase of the left boundary density results in a negative collective velocity and the perturbation does not spread into the bulk. The system has entered the maximal-current phase where it remains even if the left boundary density is further increased [8]. This phenomenon explains what may be intuitively described as the onset of an overfeeding with particles [11].

For $\beta < \frac{1}{2}$ the system does not enter the maximal-current phase (because of the negative shock velocity), but the overfeeding still occurs for $\alpha > \frac{1}{2}$ and leads to the domain wall transition $(0|1) \rightarrow (m|1)$. The overfeeding implies that further increase of the left boundary density beyond $\frac{1}{2}$ does not result in any change of the characteristic length scales in the high-density phase. This is seen in the behaviour of the domain wall velocity V (4), (5) and also in the divergence of the localization length ξ_α. The overfeeding originates in the change of sign in the collective velocity. Particle–hole symmetry can be used to extend our results to the low-density phase. Thus we can explain both the location of the second-order phase transition lines in the TASEP and the nonanalytic changes in the density profile within the low- and high-density phases.

We have performed numerical simulations of the ASEP, shown in figure 2, that give support to our ideas. We chose $N = 1000$ and on each Monte Carlo step attempted to advance the particle on a randomly chosen site (if there was one present). The initial configuration had particles placed independently and randomly, with a density step at the middle or near one end of the line. Time is measured in units of Monte Carlo steps per site. We represent the subsequent behaviour of the system by tracing the path of every 10th particle. The figure shows three cases: (a) $\alpha = \beta = 0.2$, describing a $(0|1)$ domain wall between phases that are particle–hole equivalents; (b) $\alpha = 0.3$, $\beta = 0.2$, with a $(0|1)$ domain wall between inequivalent phases; (c) $\alpha = 0.7$, $\beta = 0.2$, with a $(m|1)$ domain wall (choosing any $\alpha \geqslant 0.5$ would give exactly the same diagram). We verified that for each of these, equations (4) or (5) accurately predicted the velocity V of displacement of the wall.

4. Density profiles

We may go further and check this picture by considering the consequences of the *fluctuations* in the domain wall position. The domain wall is a compromise between the particle injection and extraction processes that attempt to enforce their distinct own stationary states. From our random walk discussion of the domain wall dynamics we expect that a superposition of the domain wall localized at the left boundary and uniform bulk density $\rho_{\rm high} = 1-\beta$ capture the physics of the high-density stationary state, in agreement with intuitive arguments [11]. For detailed analysis we adopt a coarse-grained point of view from which the motion of the domain wall essentially becomes a Poisson process. For the domain wall the combinations $j_{+,-}/(\rho_+ - \rho_-)$ which determine domain wall velocity (3) can then be interpreted as being the effective jump rates $D_{\rm R,L}$ to the right (left). Thus the diffusion constant is given by

$$D = \frac{1}{2}\frac{j_+ + j_-}{\rho_+ - \rho_-} \tag{8}$$

$$= \frac{1}{2}\frac{\beta(1-\beta)+\alpha(1-\alpha)}{1-\beta-\alpha} \qquad \text{for } \alpha, \beta < \tfrac{1}{2} \tag{9}$$

$$= \frac{4\beta(1-\beta)+1}{4(1-2\beta)} \qquad \text{for } \alpha \geqslant \tfrac{1}{2},\ \beta < \tfrac{1}{2}. \tag{10}$$

We note that equation (8) correctly reproduces the diffusion coefficient of the TASEP in an infinite system [7, 18] and that on the coexistence line $\alpha = \beta < \frac{1}{2}$, the expression reduces to $D = \alpha(1-\alpha)/(1-2\alpha)$ proposed earlier on the basis of current-fluctuation arguments [16]. On approaching the maximal current phase ($\beta \to \frac{1}{2}$) the drift velocity V vanishes but the diffusion coefficient D diverges, signalling the failure of the domain wall picture for $\beta \geqslant \frac{1}{2}$.

In the TASEP the position of a domain wall is sharp [19]. Thus it is tempting to derive the localization length which determines the decay of the density profile directly from the stationary distribution of a biased random walker in a large, but finite system. For a Poisson process with right and left hopping rates $D_{\rm R,L}$ this yields the exact equality $\xi = \ln(D_{\rm R}/D_{\rm L})$. For the domain wall motion this gives

$$\xi = |\ln(j^+/j^-)|. \tag{11}$$

Somewhat surprisingly this simple-minded ansatz is in agreement with the exact expression (1) in all phases and explains the origin of the two independent length scales $\xi_\alpha = \ln j^-$ and $\xi_\beta = \ln j^+$ in terms of the domain wall diffusion.

For a generic lattice gas we take again a coarse-grained approach and introduce a localization time τ that characterizes the length of time the wall spends away from the boundary. We argue that the drift distance $|V|\tau$ and the diffusional wandering $(D\tau)^{1/2}$ each are of the same order of magnitude as the localization length ξ itself; then $\tau \cong D/V^2$ and

$$\xi \cong D/|V|. \tag{12}$$

Thus we obtain not only a foundation in terms of the domain wall motion to the phenomenological derivation of this result by Krug [8] for the transition from the low-density phase to the maximal-current phase, but also an extension of the validity of (12) to the other phase transition lines. This domain wall approach is legitimate whenever the localization length ξ is much bigger than the (unit) lattice spacing and than other, internal bulk correlation lengths which may result from particle interactions in the lattice gas. Substituting in (12) the expressions (4), (5) and (9), (10) respectively for V and D we get expressions $\xi_{1,2}$ which are much larger than unity (and thus trustworthy) in the vicinity

of the coexistence line $\alpha = \beta < \frac{1}{2}$ (case 1) and close to the phase boundary with the maximal-current phase $\beta = \frac{1}{2}$ respectively (case 2). In these limits ξ coincides with the exact expression (11).

Finally we note that by using scaling arguments the power-law decay of the density profile in the maximal-current phase can be inferred from the superdiffusive spreading [20] of the fluctuations in the centre-of-mass of a local perturbation [8]. The same result can also be obtained from a renormalization group analysis of the TASEP with open boundaries [21].

5. Conclusions

Our domain wall approach to the determination of the phase diagram makes little reference to the microscopic details of the dynamics. The crucial ingredients, the domain wall velocity (3) and the collective velocity (7) are generally valid. We conclude that the phase diagram of the ASEP is universal in the sense that systems with a single maximum $j_{\max}$ in the current-density relation $j(\rho)$ have a similar phase diagram. Coupling to boundary reservoirs of left density $\rho_- = \alpha$ and right density ρ_+ gives a low- and a high-density phase separated by a coexistence line which is determined by $j(\rho_-) = j(\rho_+) < j_{\max}$. In the low-density phase ($j(\rho_-) < j(\rho_+)$) the bulk density equals the left boundary density ρ_-, in the high-density phase ($j(\rho_-) > j(\rho_+)$) the bulk density equals the right boundary density ρ_+. Within these phases there are domain-wall transitions at $\rho_\pm = \rho^*$ which is the density that maximizes the current and at which the collective velocity changes sign. For $\rho_+, \rho_- > \rho^*$ the system is in the maximal current phase where the bulk density takes the value ρ^*. The domain wall velocity V vanishes at all phase boundaries. Hence, given $j(\rho)$, one finds the domain wall velocity (3), the collective velocity (7) and thus the location of the phase transition lines. We argue that also equation (12) is generally valid close to the phase transition lines. Provided that the motion of the domain wall on a coarse-grained scale is a Poisson process we can then predict the shape of the density profile from the fluctuations of the domain wall motion. The diffusion coefficient D is singular along second-order lines.

This picture is well supported not only by the exact solution of the TASEP, but also by exact results on other exclusion processes [15, 22–24] for which the current-density relation and location of phase transition lines is known. Moreover, from the specific form of the current-density relations for these models we obtain from (3) and (7) new results for the domain wall velocity and collective velocity of these models. The first-order transition is consistent with the experimental data obtained for protein synthesis [2]. We note that data obtained from automobile traffic flow [25] suggest a single maximum in the current-density relation. Thus our approach may be used to predict the phase diagram of road segments between junctions where cars can enter and leave the road.

Acknowledgments

ABK has completed this work in the research group of B Widom, and was supported by the National Science Foundation and the Cornell University Materials Science Center. EBK was supported by NSF grants DMR-9412561 and DMR-9531430. We thank C L Henley and B Widom for useful discussions and M H Ernst for sending [24] prior to publication.

References

[1] Schmittmann B and Zia R K P 1995 *Phase Transitions and Critical Phenomena* vol 17, ed C Domb and J Lebowitz (London: Academic)

[2] MacDonald J T, Gibbs J H and Pipkin A C 1968 *Biopolymers* **6** 1
MacDonald J T and Gibbs J H 1969 *Biopolymers* **7** 707

[3] von Heijne G, Blomberg C and Liljenström H 1987 *J. Theor. Biol.* **125** 1
Schütz G M 1997 *Int. J. Mod. Phys.* B **11** 197

[4] Kukla V, Kornatowski J, Demuth D, Girnus I, Pfeifer H, Rees L, Schunk S, Unger K and Kärger J 1996 *Science* **272** 702

[5] Nagel K and Schreckenberg M 1992 *J. Physique* I **2** 2221
Schreckenberg M, Schadschneider A, Nagel K and Ito N 1995 *Phys. Rev.* E **51** 2339
Nagatani T 1995 *J. Phys. A: Math. Gen.* **28** 7079

[6] Ligget T 1985 *Interacting Particle Systems* (Berlin: Springer)

[7] Spohn H 1991 *Large Scale Dynamics of Interacting Particles* (New York: Springer)

[8] Krug J 1991 *Phys. Rev. Lett.* **67** 1882

[9] Andjel E D, Bramson M and Ligget T M 1988 *Prob. Theor. Relat. Fields* **78** 231

[10] Janowsky S A and Lebowitz J L 1992 *Phys. Rev.* A **45** 618
Schütz G 1993 *J. Stat. Phys.* **71** 471

[11] Schütz G and Domany E 1993 *J. Stat. Phys.* **72** 277

[12] Derrida B, Evans M R, Hakim V and Pasquier V 1993 *J. Phys. A: Math. Gen.* **26** 1493

[13] Lebowitz J L, Presutti E and Spohn H 1988 *J. Stat. Phys.* **51** 841 and references therein

[14] Derrida B, Domany E and Mukamel D 1992 *J. Stat. Phys.* **69** 667

[15] Schütz G 1993 *Phys. Rev.* E **47** 4265

[16] Derrida B, Evans M R and Mallick K 1995 *J. Stat. Phys.* **79** 833. For $\alpha = \beta$ our first example was mentioned in this reference, however, we go farther in our conclusions.

[17] Landau L D and Lifshitz E M 1981 *Physical Kinetics (Course of Theoretical Physics 10)* ed E M Lifshitz and L P Pitaevskii (New York: Pergamon)

[18] Ferrari P A and Fontes L R G 1994 *Prob. Theor. Relat. Fields* **99** 305

[19] De Masi A, Kipnis C, Presutti E and Saada E 1989 *Stoch. Stoch. Rep.* **27** 151
Ferrari P, Kipnis C and Saada E 1991 *Ann. Prob.* **19** 226

[20] van Beijeren H, Spohn H and Kutner R 1985 *Phys. Rev. Lett.* **54** 2026
van Beijeren H 1991 *J. Stat. Phys.* **63** 47

[21] Janssen H K and Oerding K 1996 *Phys. Rev.* E **53** 4544

[22] Sandow S 1994 *Phys. Rev.* E **50** 2660

[23] Rajewsky N, Santen L, Schadschneider A and Schreckenberg M 1997 *Preprint* cond-mat 9710316

[24] Tilstra L G and Ernst M H 1998 *J. Phys. A: Math. Gen.* **31** 5033. The authors have recently obtained the localization length for the ASEP with parallel update and $p = 1$. For small α, β this result is in agreement with our predictions and helped us clarify the validity of our expression for the diffusion coefficient.

[25] Hall F L, Brian L A and Gunter M A 1986 *Trans. Res.* A **20** 197